Boundary Conditions in a Multiscale Homogenization Procedure

Tomislav Lesičar, Zdenko Tonković, Jurica Sorić

Faculty of Mechanical Engineering and Naval Architecture, University of Zagreb
Ivana Lučića 5, 10000 Zagreb, Croatia

tomislav.lesicar@fsb.hr, zdenko.tonkovic@fsb.hr, jurica.soric@fsb.hr

Keywords: heterogeneous materials, multiscale, C^1 finite element, second-order computational homogenization, microfluctuations integral condition, generalized periodic boundary conditions

Abstract

This paper is concerned with a second-order multiscale computational homogenization scheme for heterogeneous materials at small strains. A special attention is directed to the macro-micro transition and the application of the generalized periodic boundary conditions on the representative volume element at the microlevel. For discretization at the macrolevel the C^1 plane strain triangular finite element based on the strain gradient theory is derived, while the standard C^0 quadrilateral finite element is used on the RVE. The implementation of a microfluctuation integral condition has been performed using several numerical integration techniques. Finally, a numerical example of a pure bending problem is given to illustrate the efficiency and accuracy of the proposed multiscale homogenization approach.

Introduction

Recently, many investigations have been reported on the methods for computing the effective mechanical properties of heterogeneous materials. Therein, multiscale techniques of modeling on multiple levels have been developed. In the multiscale micro-macro computational approach, the results obtained by the simulation of a representative volume element (RVE), employing some of the homogenization methods, are used as the input data for the model at the macrolevel. Based on the micro-macro variable dependency, the first and the second order homogenization techniques are available. The multiscale analysis using first-order computational homogenization framework includes only the first gradient of the macroscopic displacement field, retaining essential assumptions of the classical continuum mechanics. Therefore, only simple loading cases can be considered and the size effects cannot be captured. Consequently, the second-order homogenization framework, based on a non-local continuum theory, has been developed [1], [2]. It requires C^1 continuity at the macro level, which implicates discretization by a higher-order finite element, supporting higher order displacement gradients. However, the microlevel in this case can remain on C^0 continuity due to simplicity. As presented in the literature [1] and [2], an important problem in the second-order homogenization scheme is definition of the macro-micro scale transition methodology. To establish linkages between the macro- and micro-variables, due to C^1-C^0 continuity transition, an additional integral condition on the microfluctuation field should be imposed.

The main purpose of this paper is to present a new multiscale algorithm using the second-order computational homogenization scheme for a small strain case. The formulation of the C^1 continuity finite element [3] is firstly described. Then, the performance of the generalized periodic boundary conditions and various numerical integration approaches for implementation of the microfluctuation integral condition are verified. All numerical algorithms derived are implemented into FE software ABAQUS [4] using user subroutines.

Two-dimensional C^1 continuity triangular finite element

Herein, the derivation of a three-node triangular finite element with C^1 continuity for plane strain state, based on a second gradient continuum theory is presented [5]. The element, shown in Fig. 1, has 36 degrees of freedom, and approximates displacement field by the complete fifth order

polynomial. The starting point for the finite element formulation is the principle of virtual work expressed for strain gradient continuum in the following form

$$\int_A \delta\boldsymbol{\varepsilon}^T \boldsymbol{\sigma}\, \mathrm{d}A + \int_A \delta\boldsymbol{\eta}^T \boldsymbol{\mu}\, \mathrm{d}A = \int_s \delta\mathbf{u}^T \mathbf{t}\, \mathrm{d}s + \int_s \delta\left(\mathrm{grad}\,\mathbf{u}^T\right)\mathbf{T}\, \mathrm{d}s\,. \tag{1}$$

In Eq. (1), $\boldsymbol{\sigma}$ and $\boldsymbol{\mu}$ are the stress and double stress tensors, respectively. $\boldsymbol{\eta}$ represents the second-order strain tensor containing second derivatives of the displacement vector $\mathbf{u}$, while $\mathbf{T}$ is the double traction tensor, $\mathbf{T} = \boldsymbol{\tau}\mathbf{n}$. The strain and strain gradient tensors can be derived as

$$\boldsymbol{\varepsilon}^T = \left[\varepsilon_{11}\ \varepsilon_{22}\ 2\varepsilon_{12}\right] = \left[\mathbf{B}_\varepsilon\ \mathbf{v}\right]^T,\ \boldsymbol{\eta}^T = \left[\eta_{111}\ \eta_{222}\ \eta_{221}\ \eta_{122}\ 2\eta_{121}\ 2\eta_{212}\right] = \left[\mathbf{B}_\eta\ \mathbf{v}\right]^T, \tag{2}$$

where $\mathbf{B}_\varepsilon$ and $\mathbf{B}_\eta$ are the matrices containing corresponding first and second derivatives of the interpolation functions $\mathbf{N}$, and $\mathbf{v}$ represents the vector of nodal degrees of freedom. Next, in order to solve the nonlinear problem, Eq. (1) is transformed into an incremental form. Therefore, the stress increments are computed by the incremental constitutive relations as

$$\Delta\boldsymbol{\sigma} = \mathbf{C}_{\sigma\varepsilon}\Delta\boldsymbol{\varepsilon} + \mathbf{C}_{\sigma\eta}\Delta\boldsymbol{\eta},\ \Delta\boldsymbol{\mu} = \mathbf{C}_{\mu\varepsilon}\Delta\boldsymbol{\varepsilon} + \mathbf{C}_{\mu\eta}\Delta\boldsymbol{\eta}, \tag{3}$$

where $\mathbf{C}_{\sigma\varepsilon}, \mathbf{C}_{\sigma\eta}, \mathbf{C}_{\mu\varepsilon}$ and $\mathbf{C}_{\mu\eta}$ are the material tangent stiffness matrices. After some straightforward manipulation, the well-known finite element equation $\mathbf{K}\Delta\mathbf{v} = \mathbf{F}_\mathrm{e} - \mathbf{F}_\mathrm{i}$ is obtained. Herein the element stiffness matrix $\mathbf{K}$ may be decomposed in the form $\mathbf{K} = \mathbf{K}_{\sigma\varepsilon} + \mathbf{K}_{\sigma\eta} + \mathbf{K}_{\mu\varepsilon} + \mathbf{K}_{\mu\eta}$, where the particular matrices are written in the following form

$$\mathbf{K}_{\sigma\varepsilon} = \int_A \left(\mathbf{B}_\varepsilon^T \mathbf{C}_{\sigma\varepsilon} \mathbf{B}_\varepsilon\right)\mathrm{d}A,\ \mathbf{K}_{\sigma\eta} = \int_A \left(\mathbf{B}_\varepsilon^T \mathbf{C}_{\sigma\eta} \mathbf{B}_\eta\right)\mathrm{d}A,\ \mathbf{K}_{\mu\varepsilon} = \int_A \left(\mathbf{B}_\eta^T \mathbf{C}_{\mu\varepsilon} \mathbf{B}_\varepsilon\right)\mathrm{d}A,\ \mathbf{K}_{\mu\eta} = \int_A \left(\mathbf{B}_\eta^T \mathbf{C}_{\mu\eta} \mathbf{B}_\eta\right)\mathrm{d}A. \tag{4}$$

Finally, the external and internal nodal force vectors, $\mathbf{F}_\mathrm{e}$ and $\mathbf{F}_\mathrm{i}$, may be obtained from the following relations

$$\mathbf{F}_\mathrm{e} = \int_s \left(\mathbf{N}^T\mathbf{t} + \mathrm{grad}\,\mathbf{N}^T\mathbf{T}\right)\mathrm{d}s,\ \mathbf{F}_\mathrm{i} = \int_A \left(\mathbf{B}_\varepsilon^T\boldsymbol{\sigma} + \mathbf{B}_\eta^T\boldsymbol{\mu}\right)\mathrm{d}A. \tag{5}$$

The element has been implemented into the FE program ABAQUS using the user element subroutine UEL. For numerical integration of the stiffness matrix Gauss integration technique with 13 integration points has been used.

Micro-macro algorithm

In the following, the most relevant relations of the micro-macro algorithm are shown [5]. The algorithm consists of two models that represent two different levels. The first level corresponds to the macro model, discretized by the above described triangular finite elements, while the microstructural level, presented by the RVE, is discretized by the C^0 quadrilateral four-node finite elements. Here the subscript "M" denotes the macroscopic quantities, while the microscopic values are marked with the subscript "m". In each integration point of the macrolevel mesh, the RVE micro-analysis is performed. The macroscopic strain vectors $\boldsymbol{\varepsilon}_\mathrm{M}$ and $\boldsymbol{\eta}_\mathrm{M}$ are transformed into the RVE boundary nodal displacements using generalized periodic boundary conditions. After that, solving the RVE boundary value problem gives the homogenized macro stresses, $\boldsymbol{\sigma}_\mathrm{M}$ and $\boldsymbol{\mu}_\mathrm{M}$, and the constitutive matrices $\mathbf{C}_\mathrm{M}$, as shown in Fig. 2. In the second-order computational

homogenization scheme the RVE boundary displacement field is approximated by Taylor's series as

$$\mathbf{u}_{\mathrm{m}} = \mathbf{x}^T\boldsymbol{\varepsilon}_{\mathrm{M}} + 1/2\left(\mathbf{x}^T\boldsymbol{\eta}_{\mathrm{M}}\mathbf{x}\right) + \mathbf{r}\,, \tag{6}$$

where $\mathbf{x}$ is spatial coordinate on the RVE boundary, and $\mathbf{r}$ represents the microstructural fluctuation field. By exploiting the condition that the macro variables are equal to the volume average of the micro variables, the following relations are obtained

$$\frac{1}{V}\int_A\left(\mathbf{n}^T\mathbf{r}\right)\mathrm{d}A = \mathbf{0},\ \int_A\left(\mathbf{n}^T\mathbf{r}\,\mathbf{x} + \mathbf{x}^T\mathbf{r}\,\mathbf{n}\right)\mathrm{d}A = \mathbf{0}\,. \tag{7}$$

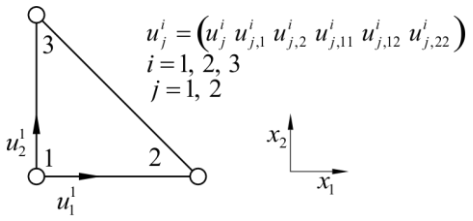

Fig. 1 C^1 triangular finite element

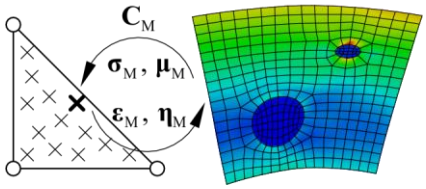

Fig. 2 Scheme of the micro-macro algorithm

For the generalized periodic boundary conditions, the second integral relation in Eq. (8) **Error! Reference source not found.** can be recast in the terms of the independent RVE boundary displacements (e. g. left and bottom)

$$\int_{A_{\mathrm{L}}}\mathbf{u}_{\mathrm{L}}\,\mathrm{d}A = \boldsymbol{\varepsilon}_{\mathrm{M}}^T\int_{A_{\mathrm{L}}}\mathbf{x}_{\mathrm{L}}\,\mathrm{d}A + \frac{1}{2}\boldsymbol{\eta}_{\mathrm{M}}\int_{A_{\mathrm{L}}}\left(\mathbf{x}_{\mathrm{L}}^T\mathbf{x}_{\mathrm{L}}\right)\mathrm{d}A,\ \int_{A_{\mathrm{B}}}\mathbf{u}_{\mathrm{B}}\,\mathrm{d}A = \boldsymbol{\varepsilon}_{\mathrm{M}}^T\int_{A_{\mathrm{B}}}\mathbf{x}_{\mathrm{B}}\,\mathrm{d}A + \frac{1}{2}\boldsymbol{\eta}_{\mathrm{M}}\int_{A_{\mathrm{B}}}\left(\mathbf{x}_{\mathrm{B}}^T\mathbf{x}_{\mathrm{B}}\right)\mathrm{d}A. \tag{9}$$

From the Hill-Mandel condition, the homogenized stress tensors are derived in the form of the surface integrals as

$$\boldsymbol{\sigma}_{\mathrm{M}} = \frac{1}{V}\int_A\left(\mathbf{p}^T\mathbf{x}\right)\mathrm{d}A \rightarrow \boldsymbol{\sigma}_{\mathrm{M}} = \frac{1}{V}\mathbf{D}\mathbf{f}_b,\ \boldsymbol{\mu}_{\mathrm{M}} = \frac{1}{2V}\int_A\left(\mathbf{x}^T\mathbf{p}\mathbf{x}\right)\mathrm{d}A \rightarrow \boldsymbol{\mu}_{\mathrm{M}} = \frac{1}{V}\mathbf{H}\mathbf{f}_b \tag{10}$$

with $\mathbf{p}$ as the surface traction, $\mathbf{D}$ and $\mathbf{H}$ representing the coordinate matrices, and $\mathbf{f}_b$ as the nodal forces of the RVE boundary nodes. Homogenized tangent matrices $\mathbf{C}_{\mathrm{M}}$ can be obtained by relating stress increments in Eq. (10) to strain increments $\Delta\boldsymbol{\varepsilon}_{\mathrm{M}}$ and $\Delta\boldsymbol{\eta}_{\mathrm{M}}$, in the form of Eq. (3). After some straightforward manipulation, the following expressions are derived

$$\mathbf{C}_{\sigma\varepsilon} = \frac{1}{V}\mathbf{D}\tilde{\mathbf{K}}_{bb}\mathbf{D}^T,\ \mathbf{C}_{\sigma\eta} = \frac{1}{V}\mathbf{D}\tilde{\mathbf{K}}_{bb}\mathbf{H}^T,\ \mathbf{C}_{\mu\varepsilon} = \frac{1}{V}\mathbf{H}\tilde{\mathbf{K}}_{bb}\mathbf{D}^T,\ \mathbf{C}_{\mu\eta} = \frac{1}{V}\mathbf{H}\tilde{\mathbf{K}}_{bb}\mathbf{H}^T, \tag{10}$$

representing the macrolevel tangent stiffness matrices in the terms of condensed RVE stiffness, $\tilde{\mathbf{K}}_{bb}$.

Numerical example

The presented micro-macro simulation algorithm has been verified on a pure bending problem. The macro model discretization and the corresponding boundary conditions are given in Fig. 3a. The material considered is an academic example of a porous steel with $E = 210$ GPa and $\nu = 0.3$, exhibiting linear isotropic hardening with the yield stress and elasto-plastic tangent modulus of 250 MPa. The RVE of the side length 0.2 mm consists of 13% randomly distributed voids of the

average radius 0.043 mm, and it is discretized by 508 quadrilateral finite elements, as shown in Fig. 3c. To enforce the pure bending state, the periodicity conditions are applied. For establishment of the straight left and right edge, the second mixed derivatives and the second derivatives of the normal displacement are suppressed. Fig. 3b shows the deformed macro model shape. The distribution of equivalent plastic strain on the deformed RVEs for a few characteristic integration points is presented in Fig. 4, where integration point (I. P.) locations on macro level are shown in Fig 3b. As can be seen in Fig 4, the deformed shapes of the RVEs correspond to their specific integration point locations. The development of microstructural shear bands between voids through plastic yielding is evident. Almost all RVE voids are finally connected through the plastic yielding bands.

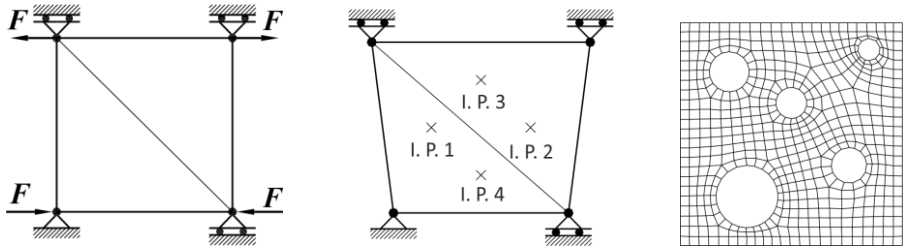

a) b) c)

Fig. 3 Pure bending problem: a) macro model with b. c., b) deformed shape, c) RVE

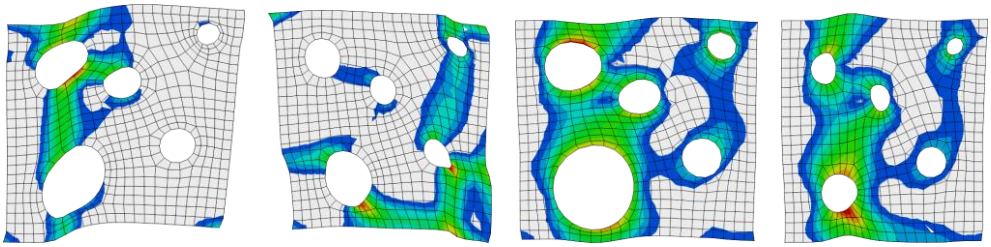

a) b) c) d)

Fig. 4 Distribution of equivalent plastic strain: a) I. P. 1, b) I. P. 2, c) I. P. 3, d) I. P. 4

Conclusions

A second-order two-scale computational homogenization procedure for modeling of heterogeneous materials at small strains is presented. For discretization of the macrolevel, the C^1 two dimensional triangular finite element is used, while the RVE is discretized by the C^0 quadrilateral finite element. The application of the generalized periodic boundary conditions and the microfluctuation integral conditions on the RVE has been investigated. The presented numerical algorithms have been implemented into FE software ABAQUS and verified on a pure bending problem. The results obtained demonstrate the accuracy and numerical efficiency of the proposed algorithms.

References

[1] Kouznetsova V.G., Geers M.G.D., Brekelmans W.A.M., Comput. Methods in Appl. Mech. and Eng., **193**:5525-5550, (2004)

[2] Kaczmarczyk L., Pearce C.J., Bićanić N., Int. J. for Numer. Methods in Eng., **74**:506-522, (2008)

[3] Lesičar T., Tonković Z., Sorić J., Čanžar P., 7th Int. Congress of Croatian Society of Mech., Zadar, (2012)

[4] Abaqus 6.10.1, Dassault Systemes

[5] Lesičar T., Tonković Z., Sorić J., submitted to the journal Comp. Mech., (2013)